

Wasserstein-Fisher-Rao Splines

Julien Clancy

clancy.julien@gmail.com

Felipe Suárez

felipesc@mit.edu

Massachusetts Institute of Technology*

April 6, 2022

Abstract

We study interpolating splines on the Wasserstein-Fisher-Rao (WFR) space of measures with differing total masses. To achieve this, we derive the covariant derivative and the curvature of an absolutely continuous curve in the WFR space. We prove that this geometric notion of curvature is equivalent to a Lagrangian notion of curvature in terms of particles on the cone. Finally, we propose a practical algorithm for computing splines extending the work of [Chewi et al. \(2020a\)](#).

1 Introduction

Let $\mu_1, \mu_2, \dots, \mu_n$ be n positive measures of differing total masses. How to interpolate them? This question is motivated by cellular trajectory reconstruction where μ_i is a population of cells at time i ([Schiebinger et al., 2019](#)). Cells move in gene space as they evolve, but also divide and proliferate. While ad-hoc fixes for this issue have been proposed, e.g. via renormalization and using optimal transport (OT) ([Chewi et al., 2020a](#)), the conservation of mass property inherent to OT makes it a less suitable tool for this task.

Curve evolution in Wasserstein space is governed by the continuity equation

$$\partial_t \mu_t + \operatorname{div}(v_t \mu_t) = 0, \quad (1)$$

which can be viewed as a simple restatement of conservation of mass, following the divergence theorem.¹ This equation is underdetermined, and the geometry of W_2 is induced by selecting for each time t the field v_t with minimal kinetic energy:

$$v_t = \arg \min_{u_t} \int \|u_t\|^2 d\mu_t = \arg \min_{u_t} \|u_t\|_{\mu_t}^2.$$

It can be seen ([Gigli, 2012](#)) that the optimal v_t lies in the closure of $\{\nabla \varphi \mid \varphi \in C_c^\infty\}$. The celebrated Benamou-Brenier theorem states that the W_2 distance, defined by optimal transport, is equal to the least total kinetic energy among all possible paths.

*J.C. was supported by NSF GRFP, and F.S. was supported by the MathWorks Fellowship and the NSF grant IIS-1838071.

¹Formally, this equation is to be interpreted weakly in duality with functions $\phi \in C_c^\infty(\mathbb{R}^d \times \mathbb{R})$ via the divergence theorem i.e. $\frac{d}{dt} \int \varphi d\mu_t = \int \langle v_t, \nabla \varphi \rangle d\mu_t$.

Theorem 1. (*Benamou and Brenier, 2000*) Let μ_0, μ_1 be probability measures. Then

$$W_2^2(\mu_0, \mu_1) = \inf_{(\mu_t, v_t)} \int_0^1 \|v_t\|_{\mu_t}^2 dt,$$

where the infimum is taken over solutions of the continuity equations with prescribed boundary data μ_0 and μ_1 .

Thus, in order to define a new metric between measures of arbitrary mass we have to alter the continuity equation, running the procedure in reverse. Turning back to intuition, where the term $\text{div}(v_t \mu_t)$ represents mass translation, we add another term representing growth or decay:

$$\partial_t \mu_t + \text{div}(v_t \mu_t) = 4\alpha_t \mu_t. \quad (2)$$

We call this the *nonconservative continuity equation*.² The term in the right-hand side allows for a *relative* growth or decay in mass. While measures (μ_t) evolving according to (2) may have varying mass, they are granted to stay positive.

From here, we measure the magnitude of a pair (v_t, α_t) by

$$\|(v_t, \alpha_t)\|_{\mu_t}^2 = \int (|v_t|^2 + 4\alpha_t^2) d\mu_t,$$

where $\|\cdot\|$ stands for norm in WFR space and $|\cdot|$ for norm of vectors in Euclidean space. The Wasserstein-Fisher-Rao distance is then defined by

$$\text{WFR}(\mu_0, \mu_1)^2 = \inf_{(\mu_t, v_t, \alpha_t)} \int_0^1 \|(v_t, \alpha_t)\|_{\mu_t}^2 dt \quad (3)$$

where, again, the minimization is over solutions to (2) with μ_0 and μ_1 prescribed. For more detailed discussions of the genesis of the equation (2) and the development of the connection with optimal transport see [Kondratyev et al., 2016](#); [Liero et al., 2018](#); [Chizat, 2017](#).

It was shown simultaneously in [Liero et al. \(2018\)](#); [Chizat \(2017\)](#) that (3) defines a metric on $\mathcal{M}_+(\mathbb{R}^d)$, the space of non-negative measures, and that it turns this into a geodesic space. Furthermore, [Kondratyev et al. \(2016\)](#) shows it has the structure of a pseudo-Riemannian manifold analogous to the Riemannian structure on W_2 ([Otto, 2001](#)), with inner product given by

$$\langle (v, \alpha), (w, \beta) \rangle_{\mu} = \int (\langle v, w \rangle + 4\alpha\beta) d\mu,$$

where the tangent space is

$$T_{\mu}(\mathcal{M}_+) = \text{clos}_{L^2(\mu)} \left\{ (\nabla \alpha, \alpha) \mid \alpha \in \mathcal{C}_c^{\infty}(\mathbb{R}^d) \right\}.$$

Remark. Notice that this is the same tangent space as for W_2 , with the difference being that the WFR Riemannian metric is the full H^1 Sobolev norm, while the W_2 Riemannian metric includes only the gradient.

There has been recent interest in understanding the curvature of these spaces ([Chewi et al., 2020b](#)), and specifically in understanding curvature-minimizing interpolating curves that generalize Euclidean splines ([Benamou et al., 2019](#); [Chen et al., 2018](#); [Chewi et al., 2020a](#)). We aim to replicate some of these advances in

²The factor of 4 is for notational convenience in accordance with the literature.

the Wasserstein-Fisher-Rao case, which, as mentioned, plays an important role in applications. Specifically, we will 1) characterize the covariant derivative in WFR space and use this to define a notion of intrinsic splines; 2) define splines from a pseudo-Eulerian perspective, as measures on paths, and establish a relationship to intrinsic splines; and 3) define a more practically workable notion of WFR splines, analogous to the transport splines of [Chewi et al. \(2020a\)](#), and examine its relationship to intrinsic splines.

2 The Covariant Derivative

In this section, we derive an expression for the covariant derivative. We first present a new derivation of the covariant derivative in W_2 that is simpler than the definition in [Gigli \(2012\)](#). In turn, this new derivation is extended to WFR space.

The Riemannian metric on W_2 is given by $\langle v, w \rangle_\mu = \int \langle v, w \rangle d\mu$, and the covariant derivative $\frac{D}{dt}$ and its associated Levi-Civita connection ∇ must satisfy two properties:

1. **Leibniz rule.** If μ_t is a curve and (v_t^1) and (v_t^2) are two (tangent) vector fields along it, then

$$\frac{d}{dt} \langle v_t^1, v_t^2 \rangle_{\mu_t} = \left\langle v_t^1, \frac{D}{dt} v_t^2 \right\rangle_{\mu_t} + \left\langle \frac{D}{dt} v_t^1, v_t^2 \right\rangle_{\mu_t}. \quad (\text{P1})$$

2. **Torsion-freeness.** If X and Y are vector fields, then

$$\nabla_X Y - \nabla_Y X = [X, Y]. \quad (\text{P2})$$

Let (v_t) be the tangent field of the curve (μ_t) (as noted above, the minimal field is unique and is a gradient³). The product rule yields

$$\begin{aligned} \frac{d}{dt} \langle v_t^1, v_t^2 \rangle_{\mu_t} &= \frac{d}{dt} \int \langle v_t^1, v_t^2 \rangle d\mu_t \\ &= \int (\langle \partial_t v_t^1, v_t^2 \rangle + \langle v_t^1, \partial_t v_t^2 \rangle) d\mu_t + \int \langle v_t^1, v_t^2 \rangle d(\partial_t \mu_t). \end{aligned}$$

Because (μ_t, v_t) solves the continuity equation, the dual definition of $\text{div}(v_t \mu_t)$ and the divergence theorem give

$$\int \langle v_t^1, v_t^2 \rangle d(\partial_t \mu_t) = \int \langle \nabla v_t^1 \cdot v_t, v_t^2 \rangle + \langle \nabla v_t^2 \cdot v_t, v_t^1 \rangle d\mu_t.$$

Together with (P1), it yields

$$\left\langle \frac{D}{dt} v_t^1, v_t^2 \right\rangle_{\mu_t} + \left\langle v_t^1, \frac{D}{dt} v_t^2 \right\rangle_{\mu_t} = \langle \partial_t v_t^1 + \nabla v_t^1 \cdot v_t, v_t^2 \rangle_{\mu_t} + \langle v_t^1, \partial_t v_t^2 + \nabla v_t^2 \cdot v_t \rangle_{\mu_t}.$$

From here, it natural to postulate that

$$\frac{D}{dt} v_t^1 = \mathcal{P}_{\mu_t} \left(\frac{D}{dt} v_t^1 \right) = \mathcal{P}_{\mu_t} (\partial_t v_t^1 + \nabla v_t^1 \cdot v_t), \quad (4)$$

where \mathcal{P}_{μ_t} is the orthogonal projection onto $T_{\mu_t}(\mathcal{P}_2)$ in $L^2(\mu_t)$. We call $\frac{D}{dt}$ the *total derivative*. Note that if $v_t^1 = v_t = \nabla \varphi_t$ then $\partial_t v_t + \nabla v_t \cdot v_t = \nabla (\partial_t \varphi_t + \frac{1}{2} |\nabla \varphi_t|^2) \in$

³In general it is merely in the closure of the set of gradients, but if all measures involved are absolutely continuous then it is truly a gradient.

$T_{\mu_t}(\mathcal{P}_2)$, so no projection is necessary, and the total and covariant derivatives coincide; in other words,

$$\frac{\mathbf{D}^2}{dt^2}\mu_t = \partial_t v_t + \nabla v_t \cdot v_t. \quad (5)$$

We now examine the torsion-free property (P2), and we follow Gigli's argument (Gigli, 2012, Section §5.1), which we partially repeat for convenience of reference. It is quite technical to give meaning directly to a smooth vector field on all of \mathcal{P}_2 , and so to the Levi-Civita connection, but it can be indirectly defined via the covariant derivative, which is all that will be necessary in this work. Let (μ_t^1) and (μ_t^2) be two absolutely continuous curves with measures that are absolutely continuous with respect to the Lebesgue measure, such that $\mu_0^1 = \mu_0^2 = \mu$, and let their velocity fields be (v_t^1) and (v_t^2) . Since v_0^1, v_0^2 are gradients, they are in $T_\mu(\mathcal{P}_2)$ for every μ , so we may define two new tangent fields along these curves by

$$\begin{aligned} u_t^1 &= v_0^2, \\ u_t^2 &= v_0^1. \end{aligned}$$

With this definition, it is reasonable to interpret

$$\nabla_{u_0^1} u_t^2 \Big|_{t=0} = \frac{\mathbf{D}}{dt} u_t^2 \Big|_{t=0},$$

with the derivative being taken along μ_t^2 , and similarly for $\nabla_{u_0^2} u_t^1$. Now, fix φ and consider the functional $F: \mu \mapsto \int \varphi d\mu$. By the continuity equation, the derivative of F along u_0^2 at μ is

$$\frac{d}{dt} F[\mu_t^1] \Big|_{t=0} = \int \varphi d(\partial_t \mu_t^1) \Big|_{t=0} = \int \langle \nabla \varphi, u_0^2 \rangle d\mu.$$

Then since the covariant derivative above respects the metric,

$$\begin{aligned} u_0^1(u_0^2(F))[\mu] &= \frac{d}{dt} \langle \nabla \varphi, u_0^2 \rangle_{\mu_t^2} \Big|_{t=0} \\ &= \left\langle \frac{\mathbf{D}}{dt} \nabla \varphi, u_0^2 \right\rangle_{\mu_t^2} + \left\langle \nabla \varphi, \frac{\mathbf{D}}{dt} u_0^2 \right\rangle_{\mu_t^2} \Big|_{t=0} \\ &= \langle \nabla^2 \varphi \cdot u_0^1, u_0^2 \rangle_\mu + \langle \nabla \varphi, \nabla_{u_0^1} u_t^2 \rangle_\mu \end{aligned}$$

where we have use the definition of $\frac{\mathbf{D}}{dt}$ to calculate $\frac{\mathbf{D}}{dt} \nabla \varphi$ on the third line. Performing the same calculation for $u_0^2(u_0^1(F))[\mu]$ and subtracting, since $\nabla^2 \varphi$ is symmetric the first terms cancel and we get

$$u_0^1(u_0^2(F))[\mu] - u_0^2(u_0^1(F))[\mu] = \left\langle \nabla \varphi, \nabla_{u_0^1} u_t^2 - \nabla_{u_0^2} u_t^1 \right\rangle_\mu$$

Since gradients $\nabla \varphi$ are dense in $T_\mu(\mathcal{P}_2)$ this means that $\frac{\mathbf{D}}{dt}$ is indeed torsion-free.

Now we repeat the argument in WFR space.

Theorem 2. *Let μ_t be an absolutely continuous curve in Wasserstein-Fisher-Rao space satisfying the continuity equation with tangent fields (v_t, α_t) . The covariant derivative is given by*

$$\frac{\mathbf{D}^2}{dt^2} \mu_t = \left(\partial_t v_t + \nabla v_t \cdot v_t + 4\alpha_t v_t \right) + \left(\partial_t \alpha_t + \frac{1}{2} |\nabla \alpha_t|^2 + 2\alpha_t^2 \right). \quad (6)$$

Proof. See appendix A. □

Theorem 2 gives a geometrical proof of the dynamical characterization of geodesics in duality with (3) (Chizat, 2017, Theorem 1.1.15; Liero et al., 2018, Theorem 8.12). Indeed, an absolutely continuous geodesic (μ_t) in WFR space with tangent $\dot{\mu}_t = (\nabla\alpha, \alpha)$ satisfies the Hamilton-Jacobi equation almost surely

$$\partial_t \alpha_t + \frac{1}{2} |\nabla \alpha_t|^2 + 2\alpha_t^2 = 0,$$

or, equivalently, the curve (μ_t) is autoparallel:

$$\nabla_{\dot{\mu}_t} \dot{\mu}_t = \frac{\mathbf{D}^2}{dt^2} \mu_t = 0. \quad (7)$$

3 E-Splines and P-splines

In this section, we define notions of E - and P -splines. As in the W_2 case, we can define an intrinsic notion of curvature-minimizing interpolators, which we term E -splines, by

$$\inf_{(\mu_t, \mathbf{v}_t)} \int_0^1 \left\| \frac{\mathbf{D}}{dt} \mathbf{v}_t \right\|_{\mu_t}^2 dt \text{ s.t. } \mu_{t_i} = \mu_i \quad (8)$$

Though the characterization (6) yields an explicit objective function, there is no practical way to optimize (8). Thus, we first define an analogy to the path splines (P -splines) introduced in Chen et al. (2018); Benamou et al. (2019). We give a brief introduction to them here (see Chewi et al., 2020a for more details).

3.1 Geodesics and P -splines in W_2

In the Wasserstein space W_2 over a metric space (\mathcal{X}, d) it is known that geodesics can be represented as measures over paths (see Lisini, 2007). Specifically, let Ω be the set all absolutely continuous paths in \mathcal{X} , let l be the length functional on Ω i.e. for $\omega \in \Omega$, $l(\omega) := \int_0^1 |\dot{\omega}_t|(t) dt$, and let e_t be the time evaluation functional at time t . If P^* is a measure over paths solution to

$$\inf_{P \in \mathcal{P}(\Omega)} \int l dP \text{ s.t. } (e_t)_\# P = \mu_t \text{ for } t \in \{0, 1\},$$

then the W_2 geodesic between μ_0 and μ_1 is given by $\mu_t = (e_t)_\# P^*$. From this starting point and in the case of $\mathcal{X} = \mathbb{R}^d$, Chen et al. (2018) define P -splines as the minimizers of

$$\inf_{P \in \mathcal{P}(\Omega)} \int c dP \text{ s.t. } (e_{t_i})_\# P = \mu_i, \quad (9)$$

where this time Ω is the set of paths with absolutely continuous derivative and c is the curvature cost $c(\omega) = \frac{1}{2} \int_0^1 |\ddot{\omega}_t|^2 dt$. Letting W_2 E -splines be defined by

$$\inf_{(\mu_t, v_t)} \int_0^1 \left\| \frac{\mathbf{D}}{dt} v_t \right\|_{\mu_t}^2 dt \text{ s.t. } \mu_{t_i} = \mu_i, \quad (10)$$

Chen et al. (2018) relates them:

Theorem 3. (Chen et al., 2018, Section 5.3) *Let (μ_t) be some curve in W_2 with derivative (v_t) . Then there is a measure $P \in \mathcal{P}(\Omega)$ such that $(e_t)_\# P = \mu_t$, and the objective in (9) is equal to that of (10). Furthermore, P can be defined from the flow maps from the continuity equation.*

This shows that problem (9) is a relaxation of (10). In Chewi et al. (2020a, Proposition 2), it is shown that this is not tight in the sense that there exists (Gaussian) measures μ_1, \dots, μ_n that are a solution to problem (10), yet are suboptimal for (9).

This formulation cannot be directly extended to WFR since, in (9), the marginals of P must have the same mass at all times. The solution is to consider curves in a different base space, introduced in Liero et al. (2016); Chizat (2017), which we briefly describe.

3.2 The Cone Space

The *cone space* \mathfrak{C} is the manifold $\mathbb{R}^d \times \mathbb{R}_+$, with $\mathbb{R}^d \times \{0\}$ identified as a single point.⁴ Points $(x, r) \in \mathfrak{C}$ are thought of as tuples of position and mass. The distance is given by

$$d_{\mathfrak{C}}((x_0, r_0), (x_1, r_1))^2 = r_0^2 + r_1^2 - 2r_0r_1 \cos(|x_0 - x_1| \wedge \pi).$$

Call the vertex of the cone (the point $\mathbb{R}^d \times \{0\}$) as \mathfrak{o} . Notice that if $|x_0 - x_1| \geq \pi$ then $d_{\mathfrak{C}}((x_0, r_0), (x_1, r_1)) = r_0 + r_1$. Since for any (x, r) we have $d_{\mathfrak{C}}((x, r), \mathfrak{o}) = r$, this reflects that fact that if x_0 and x_1 are far away then the shortest path is to the vertex and back out.

Writing $(v, p) = \frac{d}{dt}(x, r)$, the Riemannian metric on the cone space is given by

$$\langle (v_1, p_1), (v_2, p_2) \rangle_{(x, r)} = \langle v_1, v_2 \rangle r^2 + p_1 p_2. \quad (11)$$

Given a measure $\lambda \in \mathcal{M}(\mathfrak{C})$, we can project it to a measure $\mathfrak{P}\lambda \in \mathcal{M}(\mathbb{R}^d)$ via

$$\int f(x) d\mathfrak{P}\lambda(x) = \int r^2 f(x) d\lambda(x, r).$$

The measure λ is then called a lift of $\mathfrak{P}\lambda$. The presence of the term r^2 , as opposed to r , is to simplify the parametrization of \mathfrak{C} . Observe that there are many possible liftings of a measure $\mu \in \mathcal{M}(\mathbb{R}^d)$ to $\lambda \in \mathcal{M}(\mathfrak{C})$, the most obvious of which is $d\lambda(x, r) = \delta_1(r) \cdot d\mu(x)$, where $\delta_p(\cdot)$ stands for the Dirac point measure at p . As \mathfrak{C} is (save for the point \mathfrak{o}) a Riemannian manifold we can define its W_2 metric as usual

$$W_{\mathfrak{C}, 2}^2(\lambda, \eta) = \inf_{\gamma \in \Pi(\lambda, \eta)} \int d_{\mathfrak{C}}^2 d\gamma,$$

where $\Pi(\lambda, \eta)$ is the set of all couplings of measures λ and η on the cone. The following useful characterization is proved in Liero et al. (2016).

Theorem 4. (Liero et al., 2016, Theorem 7) *For any measures $\mu_0, \mu_1 \in \mathcal{M}_+(\mathbb{R}^d)$, we have*

$$\text{WFR}(\mu_0, \mu_1) = \inf_{\lambda_0, \lambda_1} W_{\mathfrak{C}, 2}(\lambda_0, \lambda_1),$$

where the $\lambda_i \in \mathcal{P}(\mathfrak{C})$ project to μ_i , $\mathfrak{P}\lambda_i = \mu_i$ for $i = 0, 1$. Furthermore, there are optimal lifts λ_0, λ_1 , and an optimal coupling γ between them.

This allows to characterize WFR geodesics in the same way as in Euclidean space.

⁴Fraktur font characters will be reserved for objects relating to the cone space, consistent with Liero et al. (2018).

Proposition 1. (*Liero et al., 2016, Section 3.4*) Let $\mu_0, \mu_1 \in \mathcal{M}_+(\mathbb{R}^d)$, and let $\gamma \in \mathcal{M}(\mathfrak{C}^2)$ be the optimal coupling of the optimal lifts in Theorem 4. For each pair of points $z_0, z_1 \in \mathfrak{C}$, let $g_t^{z_0, z_1}$ be the geodesic between them. Then the curve of measures $(\mu_t)_t$ defined by

$$\mu_t = \mathfrak{P}[(g_t^{z_1, z_2})_{\#}\gamma]$$

is a geodesic in WFR between μ_0 and μ_1 .

We may view the above theorem as saying that WFR geodesics are identified with certain measures supported on geodesics in \mathfrak{C} . In fact, [Liero et al. \(2016\)](#) prove that all curves have such a representation, and it is faithful to first order.

Theorem 5. (*Liero et al., 2016, Theorem 15*) Let (μ_t) be an absolutely continuous curve in WFR. Then there is a measure $P \in \mathcal{P}(\Omega_{\mathfrak{C}})$ such that $\mu_t = \mathfrak{P}[(e_t)_{\#}P]$ and for a.e. $t \in [0, 1]$

$$|\dot{\mu}_t|^2 = \int |\dot{z}_t|^2 dP(z)$$

where $|\dot{\mu}_t|$ is the metric derivative, which is equal to the intrinsic Riemannian quantity $\|\dot{\mu}_t\|_{\mu_t}$.

As in the W_2 case, this analogy can be extended profitably to second order—that is, to $|\ddot{\mu}_t|$ in the WFR sense.

3.3 P -Splines on WFR

In light of the dual characterization of curvature in Wasserstein space of Theorem 3 and the careful reformulation of WFR as W_2 on the cone of Proposition 1 and theorem 5, we define P -splines in WFR by

$$\inf_{P \in \mathcal{P}(\Omega_{\mathfrak{C}})} \iint_0^1 |\ddot{z}_t|^2 dt dP(z) \text{ s.t. } \mathfrak{P}[(e_{t_i})_{\#}P] = \mu_i. \quad (12)$$

We prove that this is indeed a relaxation of the E -spline problem (8).

Theorem 6. Let μ_t be a sufficiently smooth curve in WFR. Then there is a measure $P \in \mathcal{P}(\Omega_{\mathfrak{C}})$ such that $\mathfrak{P}[(e_t)_{\#}P] = \mu_t$ for all t , and the E -cost of μ is equal to the P -cost of P . The measure P is induced by the flow maps associated to the curve μ_t .

Proof. See appendix B. □

To understand the proof (and complete the description of the proposition) we must define the flow maps. In W_2 , curves of measures are interpretable as particle flows via the *flow maps* defined by

$$\dot{X}_t = v_t(X_t), X_0 = \text{Id}. \quad (13)$$

It then holds that

$$\mu_t = (X_t)_{\#}\mu_0.$$

There is a similar characterization for sufficiently smooth paths in WFR due to [Maniglia \(2007\)](#).

Proposition 2. (*Maniglia, 2007, Proposition 3.6*) Let $v \in L^1(W^{1,\infty}(\mathbb{R}^d, \mathbb{R}^d), [0, 1])$ be a vector field and $\alpha \in \mathcal{C}(\mathbb{R}^d \times [0, 1])$ a bounded locally Lipschitz scalar function. For $\mu_0 \in \mathcal{M}_+(\mathbb{R}^d)$, there is a unique weak solution to the nonconservative continuity equation (2) with initial measure μ_0 . Furthermore, this satisfies

$$\mu_t = (X_t)_\#(R_t^2 \cdot \mu_0), \quad (14)$$

for the flow map (X_t) and scalar field (R_t) which solve the ODE system

$$\begin{cases} \dot{X}_t = v_t(X_t), & X_0 = \text{Id}. \\ \dot{R}_t = 2\alpha_t(X_t) R_t, & R_0 = 1. \end{cases}$$

Analogous to what happens in the Wasserstein case, theorem 6 shows that the spline problem in Lagrangian terms can be relaxed in geometric terms via the flow map characterization of proposition 2. Thus, under absolute continuity of the measures and the curve, the Lagrangian and geometric formulations agree up to second order. The first order has three equivalent expressions, namely the metric derivative $|\dot{\mu}_t|^2$, the WFR derivative $\|\dot{\mu}_t\|_{\mu_t}^2$ and the Lagrangian form $\int |\dot{z}_t|^2 dP^*(z)$. A similar equivalence holds for the second order derivatives, i.e. the WFR covariant derivative $\|\nabla_{\dot{\mu}_t} \dot{\mu}_t\|_{\mu_t}^2$ and the Lagrangian form $\int |\ddot{z}_t|^2 dP^*(z)$. We conjecture that this equivalence holds for higher order derivatives.

4 Transport Splines

In this section, we define a tractable and smooth interpolant of measures. Piecewise linear interpolation in W_2 has the virtue of being simple to construct, which allows for additional regularization, as it is often found in applications ([Schiebinger et al., 2019](#); [Lavenant et al., 2021](#)). It yields however a curve that is not smooth. On the other hand, due to the inherent difficulty in solving the P -spline problem over W_2 , [Chewi et al. \(2020a\)](#) define a different, and substantially more tractable, interpolant that they call *transport splines*. Very briefly, they proceed as follows:

1. Start with measures μ_i at times t_i .
2. Compute the W_2 -optimal couplings $\gamma_{i \rightarrow i+1}$ from μ_i to μ_{i+1} , which are induced by maps $T_{i \rightarrow i+1}$ provided the μ_i are absolutely continuous. Let $T_i = T_{0 \rightarrow 1} \circ \dots \circ T_{i-1 \rightarrow i}$
3. Define for each x the flow map $X_t = S_t[x, T_1x, \dots, T_Nx]$, where S_t is the natural cubic spline interpolant in Euclidean space (with the base times t_i implicit).
4. Output $\mu_t = (X_t)_\# \mu_0$.

Not only is computing transport splines very fast, but if the measures μ_i are sampled from an underlying smooth curve in W_2 , then the transport spline converges in supremum norm to the true curve at rate $O(\delta^2)$, where δ is the maximum distance between successive times t_i . Importantly for applications, the curve of measure is smooth, which is not true for a piecewise-geodesic interpolant. Other virtues, and their connection with P - and E -splines, are explored in [Chewi et al. \(2020a\)](#). In this section we aim to define an analogous interpolant in WFR.

The characterization in Theorem 4 is not directly useful here, even if we knew the optimal lifts λ_0, λ_1 , it is not clear that the optimal coupling is induced by a map. Even if it were, that would not be enough for our purposes — we would want to associate a unique mass r to each initial point x , and map the position-mass pair

$(x, r(x))$ to another position-mass pair $(x', r'(x'))$, with r' the unique mass at x' . Instead we turn to a third characterization of WFR given by [Liero et al. \(2018\)](#).

Theorem 7. ([Liero et al., 2016, Theorem 8](#); [Liero et al., 2018, Theorem 6.6](#)) Let μ_0 and μ_1 be measures, and define

$$c(x, y) = -2 \log \cos(|x - y| \wedge \frac{\pi}{2}).$$

Then

$$\text{WFR}(\mu_0, \mu_1)^2 = \inf_{\eta \in \mathcal{M}_+} \text{KL}(\eta_0 \parallel \mu_0) + \text{KL}(\eta_1 \parallel \mu_1) + \int c(x, y) d\eta(x, y). \quad (15)$$

Furthermore, the infimum is achieved, and if μ_0 and μ_1 are absolutely continuous with respect to the Lebesgue measure, the optimal η^* is unique and is induced by a map.

The cost c differs from the term in the cone metric $d_{\mathcal{C}}$ by taking the minimum against $\frac{\pi}{2}$, not π . This is the difference between transport of points in \mathcal{C} and transport of measures on \mathcal{C} . To transport $z_0 = (x_0, r_0)$ to $z_1 = (x_1, r_1)$ in \mathcal{C} we may reduce the mass at x_0 to 0, then increase it again at x_1 to r_1 , whereas to transport δ_{z_0} to δ_{z_1} these can be done simultaneously (having a superposition of two deltas), so that the WFR geodesic is at each time a combination of two deltas. The superposition results in a lower overall WFR cost when $|x - y|$ is less than $\frac{\pi}{2}$.

The optimal coupling η in Theorem 7 and the optimal coupling γ in Theorem 4 are intimately related, as another theorem of [Liero et al. \(2018\)](#) shows.

Theorem 8. ([Liero et al., 2018, Theorem 6.2](#)) Suppose η minimizes the objective in Theorem 7, and let $\eta_i = \pi_i \eta$ be its marginals. Write

$$\mu_i = \sigma_i \eta_i + \mu_i^\perp$$

where $\sigma_i = d\eta_i/d\mu_i$ and μ_i is mutually singular with η_i^\perp . Define the plan γ_η by

$$\begin{aligned} d\gamma_\eta(z_0, z_1) &= \delta_{\sqrt{\sigma_0(x_0)}}(r_0) \cdot \delta_{\sqrt{\sigma_1(x_1)}}(r_1) \cdot d\eta(x_0, x_1) \\ &\quad + \delta_1(r_0) \cdot d\mu_0^\perp(x_0) \cdot \delta_\circ(z_1) + \delta_1(r_1) \cdot d\mu_1^\perp(x_1) \cdot \delta_\circ(z_0) \end{aligned}$$

Then γ_η is optimal for the objective in Theorem 4.

Now, suppose the μ_0, μ_1 are such that there $\mu_i \ll \eta_i$, so that $\mu_i^\perp = 0$ in the theorem above. This happens, for instance, when the conditions of Proposition 2 are satisfied along the geodesic between them. The optimal η for Theorem 7 is supported on a map T , and thus an optimal γ_η for Theorem 4 is supported on the assignment

$$(x_0, r_0(x_0)) \rightarrow (T(x_0), r_1(T(x_0)))$$

which associates to each x_0 a unique mass $r_0(x_0) = \sqrt{\sigma_0(x_0)}$ and maps it to another unique location and mass $r_1(T(x_0)) = \sqrt{\sigma_1(T(x_0))}$. This is much stronger than γ_η being induced by a map on \mathcal{C} .

Now, define the operator $S_t^{\mathcal{C}}[z_0, \dots, z_N]$ to be the Riemannian cubic interpolant in \mathcal{C} of the points z_0, \dots, z_N . We define *transport splines over WFR* by the following procedure

1. For each i solve (15) between μ_i and μ_{i+1} to obtain the optimal coupling $\eta_{i \rightarrow i+1}$, and thus the map $T_{i \rightarrow i+1}$. Let $T_i = T_{0 \rightarrow 1} \circ \dots \circ T_{i-1 \rightarrow i}$.

2. For each x , form a path $\tilde{X}_t(x)$ interpolating the $x_i = T_i(x)$ and a mass path $\tilde{R}_t(x)$ interpolating the masses $r_i(x_i)$.
3. Define the interpolating curve on $[t_{i-1}, t_i]$ by computing the Cone spline (X_t, R_t) with endpoint velocity constraints $\dot{X}_{t_j}(x) = \frac{d}{dt}\tilde{X}_t(x)|_{t=t_j}$ and $\dot{R}_{t_j}(x) = \frac{d}{dt}\tilde{R}_t(x)|_{t=t_j}$ for $j = i-1, i$ and $i = 1, \dots, n$.

In the first step, we obtain a family of transport maps and corresponding masses at each point x from the coupling $\eta_{i \rightarrow i+1}$. Notice that two adjacent couplings $\eta_{i-1 \rightarrow i}$ and $\eta_{i \rightarrow i+1}$ may not have the same i -th marginal, so the mass $\sqrt{\sigma_i}$ may be not uniquely defined. We remedy this by rescaling the coupling to have unit mass, so that the coupling is supported on $\sqrt{\mu_i(x_i)}$. Lifted plans on the cone are scale-invariant, thus the optimality of (15) is preserved under this scaling, as explained in Liero et al. (2016, Section §3.3). In the next step, we would ideally interpolate any sequence $(x_i, r_i)_i$ using Riemannian cubics on \mathfrak{C} , these are difficult to compute; unlike the Euclidean case, there appears to be no closed formula. We propose instead approximating the velocities at each knot from the (Euclidean) spline curves of X and R independently (Chewi et al., 2020a, Appendix D). We then solve in step 3 the cone spline problem by specifying the velocities computed in the previous step and using De Casteljau’s algorithm.

4.1 De Casteljau’s algorithm on the cone

In Euclidean space, an interpolating curve with minimal curvature is completely determined by the endpoint velocities. The De Casteljau’s algorithm computes points on this curve by iteratively finding points along the paths between the endpoints and two other control points. We describe the procedure for reference. The De Casteljau curve that interpolates x_0 and x_3 with speeds v_0 and v_3 at times $t = 0$ and $t = 1$ respectively is constructed as follows:

1. Compute control points $x_1 = x_0 + \frac{v_0}{3}$ and $x_2 = x_3 - \frac{v_3}{3}$.
2. Compute the first intermediate points $w_i(t) = (1-t)x_i + tx_{i+1}$, for $i = 0, 1, 2$.
3. Compute the second intermediate points $u_j(t) = (1-t)w_j + tw_{j+1}$, for $j = 0, 1$.
4. Compute the spline as $p(t) = (1-t)u_0 + tu_1$.

We extend this definition to the cone by replacing the linear interpolation by a geodesic interpolation (Absil et al., 2016; Gousenbourger et al., 2019). It is known that the geodesic has closed-form expression given by:

Theorem 9. (Liero et al., 2018, Section §8.1) *The geodesic interpolator of the points $z_j = (x_j, r_j)$ is given by $z(t) = (x(t), r(t))$, where*

$$\begin{aligned} x(t) &= (1 - \rho(t))x_0 + \rho(t)x_1, \\ r(t)^2 &= (1-t)^2r_0^2 + t^2r_1^2 + 2t(1-t)r_0r_1 \cos|x_0 - x_1|, \\ \rho(t) &= \frac{1}{|x_1 - x_0|} \arccos\left(\frac{(1-t)r_0 + tr_1 \cos|x_1 - x_0|}{r(t)}\right). \end{aligned}$$

Theorem 9 is only valid for distances $|x_1 - x_0| < \pi$, otherwise the geodesic simply goes from x_0 through the tip of the cone \mathfrak{o} and back to x_1 . In terms of measures, this behavior corresponds to pure growth-decay and no transport. From the discussion above about geodesics on the cone and geodesics on WFR, and because we want to model scenarios where both transport and growth are present at every moment, we restrict the computation of cone splines to points that are contained within a

ball of radius $\pi/2$. We will denote the geodesic interpolation of points z_0 and z_1 at time t as $z_0 \#_t z_1$.

In order to extend step 1 above, we must first understand how the velocities of a De Casteljau spline at $t = 0, 1$ relate to the control points x_1, x_2 .

Proposition 3. *Let (x_0, r_{x_0}) and (x_3, r_{x_3}) be given points on the cone, and (x_1, r_{x_1}) and (x_2, r_{x_2}) be control points. Let*

$$\begin{aligned} (w_i(t), r_{w_i}(t)) &:= (x_i, r_{x_i}) \#_t (x_{i+1}, r_{x_{i+1}}), \quad i = 0, 1, 2 \\ (u_j(t), r_{u_j}(t)) &:= (w_j, r_{w_j}) \#_t (w_{j+1}, r_{w_{j+1}}), \quad j = 0, 1 \\ (p(t), r_p(t)) &:= (u_0, r_{u_0}) \#_t (u_1, r_{u_1}), \end{aligned}$$

be the De Casteljau spline on the cone, then

$$\dot{p}(0) = 3 \frac{r_{x_1}}{r_{x_0}} \frac{\sin |x_0 - x_1|}{|x_0 - x_1|} (x_1 - x_0) \quad (16)$$

$$\dot{r}_p(0) = 3(r_{x_1} \cos |x_0 - x_1| - r_{x_0}) \quad (17)$$

$$\dot{p}(1) = 3 \frac{r_{x_2}}{r_{x_3}} \frac{\sin |x_3 - x_2|}{|x_3 - x_2|} (x_3 - x_2), \quad (18)$$

$$\dot{r}_p(1) = 3(r_{x_3} - r_{x_2} \cos |x_3 - x_2|). \quad (19)$$

Proof. See Appendix C. □

In particular, at an interval $[t_i, t_{i+1}]$, in order to achieve the position and mass velocities given by $v_i = \frac{d}{dt} \tilde{X}_t(x)|_{t=t_i}$ and $s_i = \frac{d}{dt} \tilde{R}_t(x)|_{t=t_i}$, we have to choose the control point (x_1, r_1) as $x_1 = x_{t_i} + c_1 \frac{v_i}{\|v_i\|}$ and $r_1 = c_2 r_{t_i}$, where c_1, c_2 are solved from (16-17):

$$\begin{aligned} c_1 &= \arctan \left(\frac{\|v_i\|}{\frac{s_i}{r_{t_i}} + 3\delta^{-1}} \right), \\ c_2 &= \frac{\delta}{3} \sqrt{\|v_i\|^2 + \left(\frac{s_i}{r_{t_i}} + 3\delta^{-1} \right)^2}, \end{aligned}$$

where $\delta = t_{i+1} - t_i$. Similarly for t_{i+1} , we choose (x_2, r_2) with $x_2 = x_{t_{i+1}} - c_3 \frac{v_{i+1}}{\|v_{i+1}\|}$, $r_2 = c_4 r_{t_{i+1}}$, and solve (18-19):

$$\begin{aligned} c_3 &= \arctan \left(\frac{\|v_{i+1}\|}{3\delta^{-1} - \frac{s_{i+1}}{r_{t_{i+1}}}} \right), \\ c_4 &= \frac{\delta}{3} \sqrt{\|v_{i+1}\|^2 + \left(3\delta^{-1} - \frac{s_{i+1}}{r_{t_{i+1}}} \right)^2}. \end{aligned}$$

The derivation of the above equations requires that $c_1, c_3 \geq 0$; it reflects the fact that $x_1 - x_0$ and $x_3 - x_2$ point in the right direction. This translates to $s_i \geq -3\delta^{-1} r_{t_i}$ and $s_{i+1} \leq 3\delta^{-1} r_{t_{i+1}}$, which constraints the possible velocities that are achievable by the De Casteljau's algorithm. To comprehend why this happens, notice that unlike the Euclidean case, the second variable r is constrained to be non-negative. This limits the possible masses of the control points x_1, x_2 , which in turn limits the endpoint derivatives $\dot{r}_p(0)$ and $\dot{r}_p(1)$ (equations (17),(19)).

There are two limitations to the cone transport spline problem: the maximum $\frac{\pi}{2}$ diameter in the position space and the bounds in knot velocities in mass space, as described above. Furthermore, the velocities are estimated from two independent spline problems. A simple solution to these limitations is to 1) scale down all distances to a space with a smaller diameter and 2) scale up the knot times to allow for smaller endpoint derivatives.

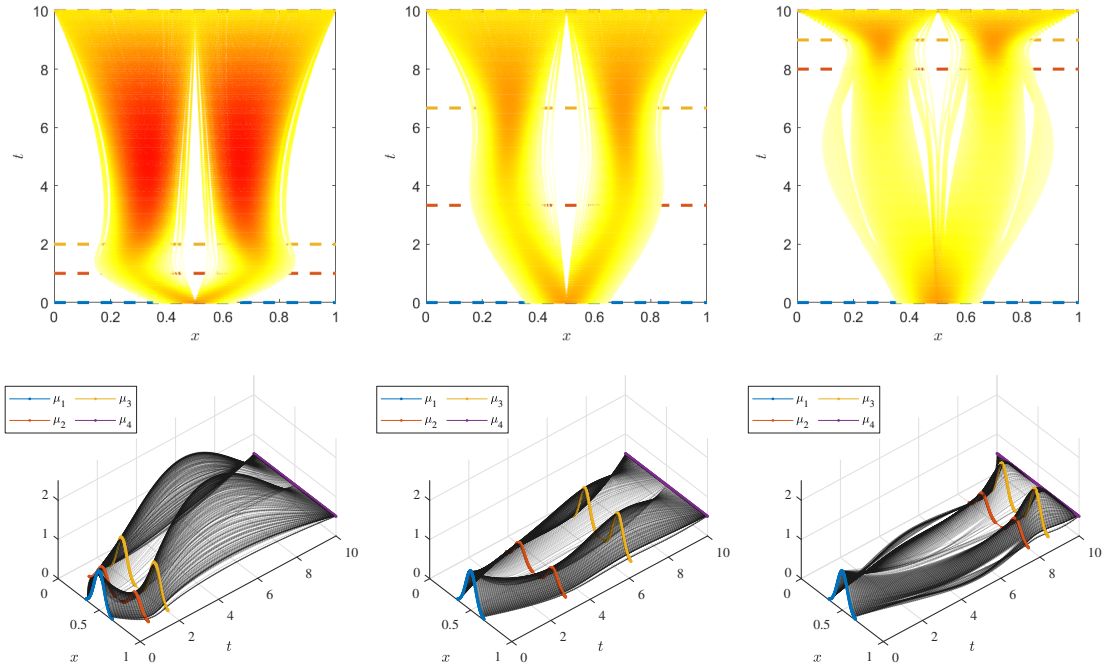


Figure 1: De Casteljau cone interpolation of measures μ_1, \dots, μ_4 . Measure values are shown as a heat map (top) and in a three-dimensional plot (bottom) as a function of time. Knot times (t_1, \dots, t_4) are $(0, 1, 2, 10)$ (left), $(0, \frac{10}{3}, \frac{20}{3}, 10)$ (center), and $(0, 8, 9, 10)$ (right). $\sigma = 0.06$.

5 Numerical Experiments

In this section, we illustrate the behavior of the cone transport spline via the De Casteljau’s algorithm. We showcase different aspects of the paths qualitatively by considering spline interpolation of measures in one and two dimensions. In section 5.1 we consider interpolation with varying times. We show in section 5.2 two alternative ways of solving a spline problem given by discrete measures by considering a problem in two dimensions.⁵

5.1 Time effects and Linear interpolation

In this subsection, we look at the effects of time distribution of knots for a one dimensional cone spline problem. The map obtained from solving (7) is induced by a map only when the measures are absolutely continuous with respect to the Lebesgue measure. Indeed, the WFR plan from a single particle to two particles cannot be induced by a map. The same effect is present when solving problem (7) computationally. Here we choose to solve problem (7) using entropic regularization (Chizat et al., 2018; Peyré et al., 2019) and derive an approximation of the map from its solution by taking expectation⁶ of the marginals: $T(x) = \mathbb{E}_\eta[y|x]$, inspired by Pooladian and Niles-Weed (2021).

Let $\gamma_\sigma(x) = \exp(-\frac{1}{2\sigma^2}x^2)\mathbb{1}_{[-2,2]}(x/\sigma)$. For our first experiment, we interpolate the measures

$$d\mu_1(x) = \gamma_\sigma\left(x - \frac{1}{2}\right) dx,$$

⁵The MATLAB code used for generating the figures can be found here https://github.com/felipesua/WFR_splines.

⁶We can assume η is a probability measure by the scale invariance property of the projection from the cone.

$$\begin{aligned}
d\mu_2(x) &= \frac{1}{2} (\gamma_\sigma(x - 0.3) + \gamma_\sigma(x - 0.7)) dx, \\
d\mu_3(x) &= (\gamma_\sigma(x - 0.3) + \gamma_\sigma(x - 0.7)) dx, \\
d\mu_4(x) &= \frac{1}{2} \mathbb{1}_{[0,1]}(x) dx,
\end{aligned}$$

which we interpolate at three set of knot times (t_1, \dots, t_4) : $(0, 1, 2, 10)$, $(0, \frac{10}{3}, \frac{20}{3}, 10)$, and $(0, 8, 9, 10)$ in figure 1.

5.2 Space discretization

We give details for the interpolation of measures in two dimensions in figure 2. For this example suppose we want to interpolate a set of particles. Since we need to represent them as absolutely continuous measures to be able to obtain a map, we convolve with a kernel and discretize the domain like in the previous section. As noted by Lavenant et al. (2021), gridding grows exponentially with the dimension which makes it infeasible for high-dimensional applications. We show here the result of fine gridding and compare it to sampling uniformly from the support.

Suppose the resulting interpolating measures are as follows. Let

$$\gamma_\sigma(x) = \exp(-\frac{1}{2\sigma^2}\|x\|^2) \mathbb{1}_{B_2(0)}(x).$$

We interpolate

$$\begin{aligned}
d\mu_1(x) &= \frac{3}{4} \gamma_{2\sigma}(x) dx, \\
d\mu_2(x) &= 0.65 \left(\gamma_\sigma(x - (\frac{\sqrt{2}}{20}, \frac{\sqrt{2}}{20})) + \gamma_\sigma(x - (0, -\frac{\sqrt{2}}{20})) + \gamma_\sigma(x - (\frac{\sqrt{2}}{20}, -\frac{\sqrt{2}}{20})) \right) dx, \\
d\mu_3(x) &= \frac{3}{4} \left(\gamma_\sigma(x - (\frac{3}{20}, \frac{3}{20})) + \gamma_\sigma(x - (\frac{3}{20}, -\frac{3}{20})) \right) dx, \\
d\mu_4(x) &= \gamma_{2\sigma}(x - (\frac{1}{5}, 0)) dx.
\end{aligned}$$

Acknowledgements

We thank Philippe Rigollet and Sinho Chewi for helpful comments and suggestions on the manuscript.

A Derivation of the covariant derivative

Theorem 2. *Let μ_t be an absolutely continuous curve in Wasserstein-Fisher-Rao space satisfying the continuity equation with tangent fields (v_t, α_t) . The covariant derivative is given by*

$$\frac{\mathbf{D}^2}{dt^2} \mu_t = \begin{pmatrix} \partial_t v_t + \nabla v_t \cdot v_t + 4\alpha_t v_t \\ \partial_t \alpha_t + \frac{1}{2} |\nabla \alpha_t|^2 + 2\alpha_t^2 \end{pmatrix}. \quad (6)$$

Proof. Let $\mathbf{u}_t^i = (u_t^i, \beta_t^i)$ be two tangent fields along a curve μ_t , which has derivative (v_t, α_t) . Metric compatibility then reads

$$\begin{aligned}
\frac{d}{dt} \langle \mathbf{u}_t^1, \mathbf{u}_t^2 \rangle_{\mu_t} &= \int \langle \partial_t u_t^1, u_t^2 \rangle + \langle u_t^1, \partial_t u_t^2 \rangle + 4\partial_t \beta_t^1 \beta_t^2 + 4\beta_t^1 \partial_t \beta_t^2 d\mu_t \\
&\quad + \int \langle u_t^1, u_t^2 \rangle + 4\beta_t^1 \beta_t^2 d(\partial_t \mu_t) \\
&= T_1 + T_2
\end{aligned}$$

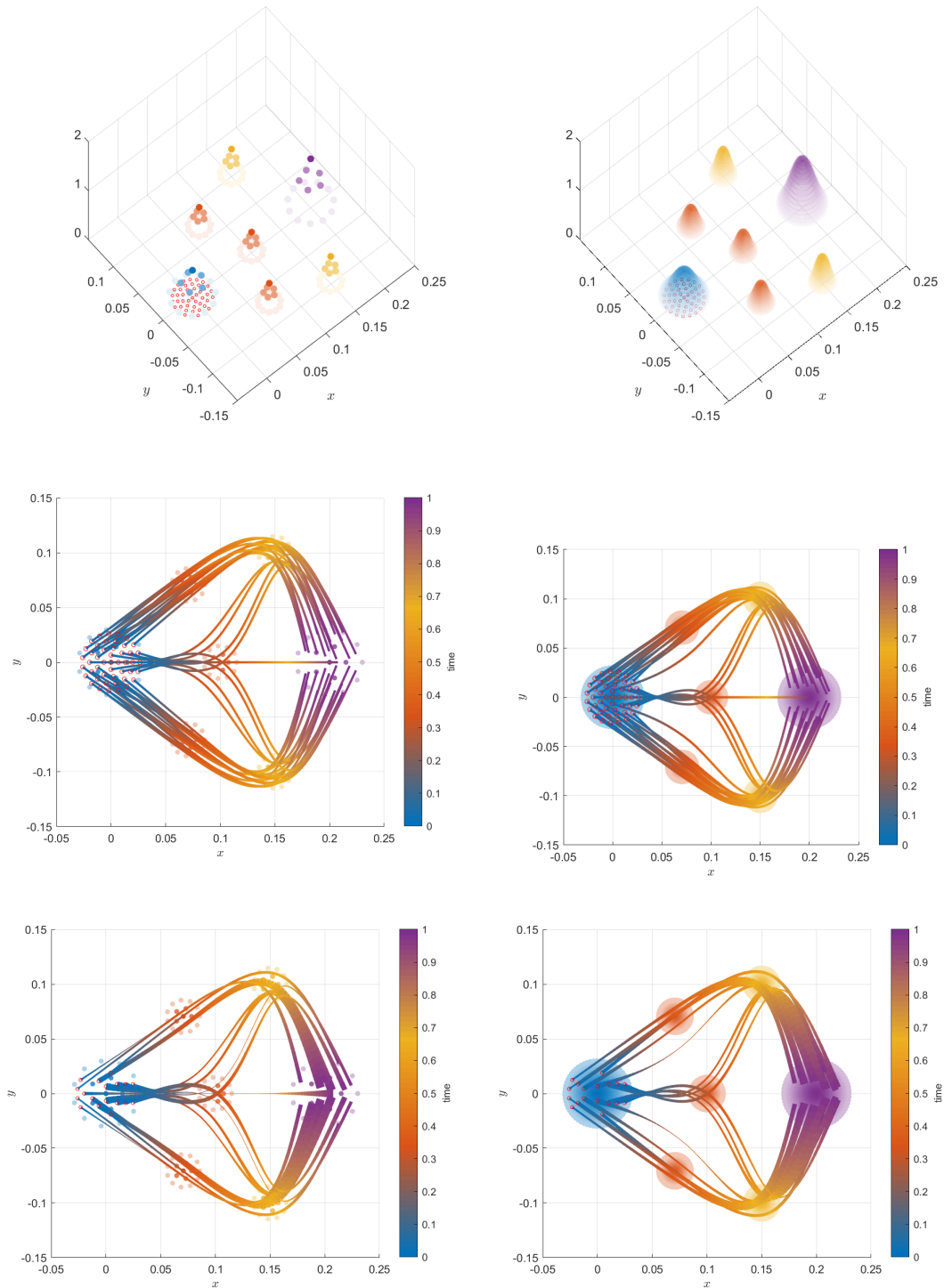


Figure 2: Subsampled (left) and gridded (right) interpolating measures. Measures μ_1, \dots, μ_4 are shown in blue, orange, yellow, and purple respectively (top). Interpolated paths are computed for the points shown in red (middle) as a function of time varying by color. The width of select curves is changed according to the value of the measure (bottom). $\sigma = 0.01$

By the continuity equation and the dual definition of $\text{div } v_t \mu_t$, the second integral becomes

$$\begin{aligned} T_2 &= \int \langle \nabla u_t^1 \cdot v_t, u_t^2 \rangle + \langle u_t^2, \nabla u_t^2 \cdot v_t \rangle + 4\alpha_t \langle u_t^1, u_t^2 \rangle \\ &\quad + \int 4\beta_t^2 \langle \nabla \beta_t^1, v_t \rangle + 4\beta_t^1 \langle \nabla \beta_t^2, v_t \rangle + 16\alpha_t \beta_t^1 \beta_t^2 d\mu_t \end{aligned}$$

Now, we need this to be equal to $\langle \mathbf{u}_t^1, \frac{\mathbf{D}}{dt} \mathbf{u}_t^2 \rangle + \langle \frac{\mathbf{D}}{dt} \mathbf{u}_t^1, \mathbf{u}_t^2 \rangle$. Some terms are uniquely attributable to one or the other, such as $\int \langle \partial_t u_t^1, u_t^2 \rangle$, but some are not, such as $4\beta_t^2 \langle \nabla \beta_t^1, v_t \rangle$. This can arise from either of the two terms: as $\nabla \beta_t^i = u_t^i$,

$$\langle (0, \langle \nabla \beta_t^1, v_t \rangle), \mathbf{u}_t^2 \rangle_{\mu_t} = \langle \mathbf{u}_t^1, (4\beta_t^2 v, 0) \rangle_{\mu_t}$$

Indeed, by splitting these terms and gathering the others, the possible covariant derivatives that satisfy metric compatibility are of the form

$$\frac{\mathbf{D}}{dt} \mathbf{u}_t = \mathcal{P}_{\mu_t} \begin{pmatrix} \partial_t u_t + \nabla u_t \cdot v_t + 2\alpha_t u_t + 4p\beta_t v_t \\ \partial_t \beta_t + (1-p) \langle \nabla \beta_t, v_t \rangle + 2\alpha_t \beta_t \end{pmatrix}$$

for real p . Let us check the torsion-free identity with $p = 1/2$. In this case, if $\mathbf{u}_t = (\nabla \varphi, \varphi)$ is constant in time, then

$$\frac{\mathbf{D}}{dt} \begin{pmatrix} \nabla \varphi \\ \varphi \end{pmatrix} = \mathcal{P}_{\mu_t} \begin{pmatrix} \nabla^2 \varphi \cdot v_t + 2\alpha_t \nabla \varphi + 2\varphi v_t \\ \frac{1}{2} \langle \nabla \varphi, v_t \rangle + 2\alpha_t \varphi \end{pmatrix}$$

Now, with the setup as in the W_2 case, defining $F: \varphi \mapsto \int \varphi d\mu$ and writing $\varphi = (\nabla \varphi, \varphi)$, we have from the continuity equation

$$\partial_t F[\mu_t^i] = \int \langle \varphi, \mathbf{v}_t^i \rangle d\mu_t^i$$

where \mathbf{v}_t^i is the derivative of μ_t^i . As above, we have

$$\begin{aligned} \mathbf{u}_0^1(\mathbf{u}^2(F))[\mu] &= \frac{d}{dt} \langle \varphi, \mathbf{u}_t^2 \rangle_{\mu_t^2} \Big|_{t=0} \\ &= \left\langle \frac{\mathbf{D}}{dt} \varphi, \mathbf{u}_t^2 \right\rangle_{\mu_t^2} + \left\langle \varphi, \nabla_{\mathbf{u}_0^1} \mathbf{u}_t^2 \right\rangle_{\mu_t^2} \Big|_{t=0} \end{aligned}$$

Recalling that at $t = 0$ we have $\mathbf{u}_0^2 = \mathbf{v}_0^1 = (v_0^1, \alpha_0^1)$, the first term becomes (we may ignore the projection, since \mathbf{u}_t^2 is already tangent)

$$Q_1 = \left\langle \begin{pmatrix} \nabla^2 \varphi \cdot v_0^2 + 2\alpha_0^2 \nabla \varphi + 2\varphi v_0^2 \\ \frac{1}{2} \langle \nabla \varphi, v_0^2 \rangle + 2\alpha_0^2 \varphi \end{pmatrix}, \begin{pmatrix} v_0^1 \\ \alpha_0^1 \end{pmatrix} \right\rangle_{\mu}$$

while the corresponding term from $\mathbf{u}_0^2(\mathbf{u}^2(F))[\mu]$ is

$$Q_2 = \left\langle \begin{pmatrix} \nabla^2 \varphi \cdot v_0^1 + 2\alpha_0^1 \nabla \varphi + 2\varphi v_0^1 \\ \frac{1}{2} \langle \nabla \varphi, v_0^1 \rangle + 2\alpha_0^1 \varphi \end{pmatrix}, \begin{pmatrix} v_0^2 \\ \alpha_0^2 \end{pmatrix} \right\rangle_{\mu}$$

and we must check that these agree. The “top-left”, “top-right”, and “bottom-right” terms are identical for both. The top-middle of the first is equal to the bottom-left for the second, and vice-versa. Thus we have shown that the covariant derivative is given by

$$\frac{\mathbf{D}}{dt} \mathbf{u}_t = \mathcal{P}_{\mu_t} \begin{pmatrix} \partial_t u_t + \nabla u_t \cdot v_t + 2\alpha_t u_t + 2\beta_t v_t \\ \partial_t \beta_t + \frac{1}{2} \langle \nabla \beta_t, v_t \rangle + 2\alpha_t \beta_t \end{pmatrix}$$

and in specific,

$$\frac{\mathbf{D}^2}{dt^2} \mu_t = \begin{pmatrix} \partial_t v_t + \nabla v_t \cdot v_t + 4\alpha_t v_t \\ \partial_t \alpha_t + \frac{1}{2} |\nabla \alpha_t|^2 + 2\alpha_t^2 \end{pmatrix} \quad (20)$$

This quantity is tangent, so no projection is necessary. \square

B Proof of equivalence in curvature

Theorem 6. *Let μ_t be a sufficiently smooth curve in WFR. Then there is a measure $P \in \mathcal{P}(\Omega_{\mathfrak{C}})$ such that $\mathfrak{P}[(e_t)_{\#}P] = \mu_t$ for all t , and the E -cost of μ is equal to the P -cost of P . The measure P is induced by the flow maps associated to the curve μ_t .*

Proof. Making the definition explicit, we wish of our measure P that the cost of (12) is equal to

$$\int_0^1 \int |\partial_t v_t + \nabla v_t \cdot v_t + 4\alpha_t v_t|^2 + 4 \left(\partial_t \alpha_t + \frac{1}{2} |\nabla \alpha_t|^2 + 2\alpha_t^2 \right)^2 d\mu_t dt \quad (21)$$

Let $\lambda_0 \in \mathcal{P}(\mathfrak{C})$ be a lift of μ_0 . By Proposition 2, the measure $\lambda_t = (X_t, R_t)_{\#} \lambda_0$ is a lift of μ_t .

In order to compute the covariant derivative of a curve on the cone, we compute the Christoffel symbols. These are given by the formulas

$$\nabla_{\partial x_i} \partial x_j = \Gamma_{ij}^k \partial_k, \quad \Gamma_{ij}^k = \frac{1}{2} g^{kl} \left(\frac{\partial}{\partial_j} g_{il} + \frac{\partial}{\partial_i} g_{jl} - \frac{\partial}{\partial_l} g_{ij} \right).$$

Let $\partial x_1, \dots, \partial x_n, \partial_r$ be the coordinate basis of the tangent space on the cone, hence

$$(g_{ij})_{ij} = \begin{pmatrix} r^2 I_n & 0 \\ 0 & 1 \end{pmatrix}, \quad \frac{\partial}{\partial_k} g_{ij} = \begin{cases} 2r & i = j \neq r, k = r, \\ 0, & \text{else.} \end{cases}$$

Since (g^{ij}) and $\partial_r g_{ij}$ are only defined along the diagonal and $\partial_l g_{ij} = 0$ for $l \neq r$, the only terms that do not vanish are

$$\Gamma_{rj}^k = r^{-1} \delta_{jk}, \quad \Gamma_{ij}^r = -r \delta_{ij}$$

thus the Levi-Civita connection on the cone is given by

$$\nabla_{\partial_r} \partial_r = 0, \quad \nabla_{\partial_r} X = r^{-1} X, \quad \nabla_{X_1} X_2 = -r \langle X_1, X_2 \rangle \partial_r.$$

From this, the covariant derivative of a curve $z_t = (x_t, r_t)$ on the cone is given by

$$\ddot{z}_t = \nabla_{\dot{z}_t} \dot{z}_t = \left(\ddot{x}_t + 2 \frac{\dot{r}_t}{r_t} \dot{x}_t, \ddot{r}_t - r_t |\dot{x}_t|^2 \right)$$

thus from the Riemannian metric (11)

$$|\ddot{z}_t|^2 = |r_t \ddot{x}_t + 2 \dot{r}_t \dot{x}_t|^2 + |\ddot{r}_t - r_t |\dot{x}_t|^2|^2$$

Let λ_0 be any lift of μ_0 and define P to place mass $\lambda_0(z_0)$ on the path $z_t = (X_t(x_0), R_t(r_0))$, so that P is supported on the flow map curves in $\Omega_{\mathfrak{C}}$. By applying the total derivative to the defining equations of the flow maps, these curves satisfy

$$\begin{aligned} \dot{x}_t &= v_t(x_t) \\ \ddot{x}_t &= \partial_t v_t + \nabla v_t \cdot v_t \\ \dot{r}_t &= 2r_t \alpha_t(x_t) \\ \ddot{r}_t &= 2r_t (\partial_t \alpha_t + \nabla \alpha_t \cdot v_t + 2\alpha_t^2) \end{aligned}$$

Now, we have

$$\int_{\Omega_{\mathfrak{C}}} \int_0^1 |\ddot{z}_t|^2 dt dP(z) = \int_{\mathfrak{C}} \int_0^1 |\ddot{z}_t|^2 dt d\lambda_0(z_0)$$

Expanding out, this is

$$\int_{\mathcal{E}} \int_0^1 |r_t \ddot{x}_t + 2\dot{r}_t \dot{x}_t|^2 + |\ddot{r}_t - r_t |\dot{x}_t|^2|^2 dt d\lambda_0(z_0)$$

Let us deal with each term separately so the expressions do not become unwieldy. For the first

$$\begin{aligned} & \int_{\mathcal{E}} \int_0^1 |r_t \ddot{x}_t + 2\dot{r}_t \dot{x}_t|^2 dt d\lambda_0(z_0) \\ &= \int_{\mathcal{E}} \int_0^1 r_t^2 |\partial_t v_t + \nabla v_t \cdot v_t + 4\alpha_t v_t|^2(x_t) dt d\lambda_0(z_0) \\ &= \int_0^1 \int_{\mathcal{E}} |\partial_t v_t + \nabla v_t \cdot v_t + 4\alpha_t v_t|^2(x_t) d(r_t^2 \cdot \lambda_0)(z_0) dt \\ &= \int_0^1 \int_{\mathcal{E}} |\partial_t v_t + \nabla v_t \cdot v_t + 4\alpha_t v_t|^2(x) d\mu_t(x) dt \end{aligned}$$

We have used that $(X_t, R_t) \# \lambda_0 = \lambda_t$ and $\mathfrak{P}\lambda_t = \mu_t$. The second term is dealt with in exactly the same way,

$$\begin{aligned} & \int_{\mathcal{E}} \int_0^1 |\ddot{r}_t - r_t |\dot{x}_t|^2|^2 dt d\lambda_0(z_0) \\ &= \int_{\mathcal{E}} \int_0^1 4r_t^2 |\partial_t \alpha_t + \frac{1}{2} \nabla \alpha_t \cdot v_t + 2\alpha_t^2|^2(x_t) dt d\lambda_0(z_0) \\ &= \int_0^1 \int_{\mathcal{E}} 4 |\partial_t \alpha_t + \frac{1}{2} \nabla \alpha_t \cdot v_t + 2\alpha_t^2|^2(x_t) d(r_t^2 \cdot \lambda_0)(z_0) dt \\ &= \int_0^1 \int_{\mathcal{E}} 4 |\partial_t \alpha_t + \frac{1}{2} \nabla \alpha_t \cdot v_t + 2\alpha_t^2|^2(x_t) d\mu_t(x) dt. \end{aligned}$$

□

C Cone De Casteljau's algorithm

Proposition 3. *Let (x_0, r_{x_0}) and (x_3, r_{x_3}) be given points on the cone, and (x_1, r_{x_1}) and (x_2, r_{x_2}) be control points. Let*

$$\begin{aligned} (w_i(t), r_{w_i}(t)) &:= (x_i, r_{x_i}) \#_t (x_{i+1}, r_{x_{i+1}}), \quad i = 0, 1, 2 \\ (u_j(t), r_{u_j}(t)) &:= (w_j, r_{w_j}) \#_t (w_{j+1}, r_{w_{j+1}}), \quad j = 0, 1 \\ (p(t), r_p(t)) &:= (u_0, r_{u_0}) \#_t (u_1, r_{u_1}), \end{aligned}$$

be the De Casteljau spline on the cone, then

$$\dot{p}(0) = 3 \frac{r_{x_1} \sin |x_0 - x_1|}{r_{x_0} |x_0 - x_1|} (x_1 - x_0) \quad (16)$$

$$\dot{r}_p(0) = 3(r_{x_1} \cos |x_0 - x_1| - r_{x_0}) \quad (17)$$

$$\dot{p}(1) = 3 \frac{r_{x_2} \sin |x_3 - x_2|}{r_{x_3} |x_3 - x_2|} (x_3 - x_2), \quad (18)$$

$$\dot{r}_p(1) = 3(r_{x_3} - r_{x_2} \cos |x_3 - x_2|). \quad (19)$$

Proof. Let $\theta_i := |x_{i+1} - x_i|$. Since the expressions for w , u and P are all the same with different interpolating points, we compute the derivatives of w , ρ , r and θ

with the suscripts removed. To compute each derivative, we just replace with the corresponding suscript.

For $\theta = |x_1 - x_0|$,

$$\theta\dot{\theta} = \langle x_1 - x_0, \dot{x}_1 - \dot{x}_0 \rangle.$$

For a point $w_0 = (1 - \rho)x_0 + \rho x_1$,

$$\dot{w}_0 = (x_1 - x_0)\dot{\rho} + (1 - \rho)\dot{x}_0 + \rho\dot{x}_1. \quad (22)$$

For the mass $r^2 = r_0^2(1 - t)^2 + r_1^2 t^2 + 2r_0 r_1 t(1 - t) \cos(\theta)$,

$$\begin{aligned} r\dot{r} = & 2r_0\dot{r}_0(1 - t)^2 - r_0^2(1 - t) + r_1\dot{r}_1 t^2 + r_1^2 t \\ & + (\dot{r}_1 r_0 + \dot{r}_0 r_1)t(1 - t) \cos(\theta) \\ & + r_0 r_1(1 - 2t) \cos(\theta) - r_0 r_1 t(1 - t) \sin(\theta)\dot{\theta}. \end{aligned} \quad (23)$$

For the local time $\rho = \frac{1}{\theta} \arccos\left(\frac{r_0(1-t)+r_1 t \cos(\theta)}{r}\right)$,

$$\begin{aligned} \dot{\rho}\theta + \rho\dot{\theta} = & \frac{1}{r_{w_0}^2} ((1 - t)t \sin(\theta)(\dot{r}_1 r_0 - \dot{r}_0 r_1) \\ & + (1 - t)t \cos(\theta)r_0 r_1 \dot{\theta} \\ & + r_0 r_1 \sin(\theta) + r_1^2 \dot{\theta} t^2). \end{aligned} \quad (24)$$

For the first interpolation points w_0, w_1, w_2 we have in particular that $\dot{x}_i, \dot{r}_{x_i} = 0$, hence

$$\begin{aligned} \dot{\theta}_{w_i} &= 0, \\ \dot{w}_i &= (x_{i+1} - x_i)\dot{\rho}_{w_i}, \\ \dot{r}_{w_i} &= \frac{1}{r_{w_i}} \left(-r_{x_i}^2(1 - t) + r_{x_{i+1}}^2 t + r_{x_i} r_{x_{i+1}}(1 - 2t) \cos(\theta_{w_i}) \right), \\ \dot{\rho}_{w_i} &= \frac{r_{x_i} r_{x_{i+1}}}{\theta_{w_i}} \sin(\theta_{w_i}) - \rho_{w_i} \frac{\dot{\theta}_{w_i}}{\theta_{w_i}}. \end{aligned}$$

Thus at $t = 0$,

$$\dot{\theta}_{w_i}(0) = 0 \quad (25)$$

$$\dot{\rho}_{w_i}(0) = \frac{r_{x_{i+1}}}{r_{x_i}} \frac{\sin(\theta_i)}{\theta_i} \quad (26)$$

$$\dot{r}_{w_i}(0) = r_{x_{i+1}} \cos(\theta_i) - r_{x_i} \quad (27)$$

$$\dot{w}_i(0) = (x_{i+1} - x_i) \frac{r_{x_{i+1}}}{r_{x_i}} \frac{\sin(\theta_i)}{\theta_i} \quad (28)$$

and $t = 1$,

$$\dot{\theta}_{w_i}(1) = 0 \quad (29)$$

$$\dot{\rho}_{w_i}(1) = \frac{r_{x_i}}{r_{x_{i+1}}} \frac{\sin(\theta_i)}{\theta_i} \quad (30)$$

$$\dot{r}_{w_i}(1) = r_{x_{i+1}} - r_{x_i} \cos(\theta_i) \quad (31)$$

$$\dot{w}_i(1) = (x_{i+1} - x_i) \frac{r_{x_i}}{r_{x_{i+1}}} \frac{\sin(\theta_i)}{\theta_i}. \quad (32)$$

We substitute these expression back into the formulas for the derivatives of position (22), mass (23) and local time (24) for u_j and p , for $j = 0, 1$. Notice that for both $t = 0$ and $t = 1$ the dependence on θ vanishes.

$$\dot{\rho}_{u_j}(0) = \frac{r_{x_{j+1}} \sin(\theta_j)}{r_{x_j} \theta_j} \quad (33)$$

$$\dot{r}_{u_j}(0) = 2 (r_{x_{j+1}} \cos(\theta_j) - r_j) \quad (34)$$

$$\dot{u}_j(0) = 2(x_{j+1} - x_j) \frac{r_{x_{j+1}} \sin(\theta_j)}{r_{x_j} \theta_j} \quad (35)$$

$$\dot{\rho}_{u_j}(1) = \frac{r_{x_j} \sin(\theta_{j+1})}{r_{x_{j+1}} \theta_{j+1}} \quad (36)$$

$$\dot{r}_{u_j}(1) = 2 (r_{x_{j+1}} - r_{x_j} \cos(\theta_{j+1})) \quad (37)$$

$$\dot{u}_j(1) = 2(x_{j+1} - x_j) \frac{r_{x_{j+1}} \sin(\theta_{j+1})}{r_{x_j} \theta_{j+1}} \quad (38)$$

Finally for p ,

$$\dot{\rho}_p(0) = \frac{r_{x_1} \sin(\theta_0)}{r_{x_0} \theta_0}, \quad (39)$$

$$\dot{r}_p(0) = 3 (r_{x_1} \cos(\theta_0) - r_{x_0}), \quad (40)$$

$$\dot{p}(0) = 3(x_1 - x_0) \frac{r_{x_1} \sin(\theta_0)}{r_{x_0} \theta_0}, \quad (41)$$

$$\dot{\rho}_p(1) = \frac{r_{x_2} \sin(\theta_2)}{r_{x_3} \theta_2}, \quad (42)$$

$$\dot{r}_p(1) = 3 (r_{x_3} - r_{x_2} \cos(\theta_2)), \quad (43)$$

$$\dot{p}(1) = 3(x_3 - x_2) \frac{r_{x_2} \sin(\theta_2)}{r_{x_3} \theta_2}. \quad (44)$$

□

References

- Absil, P.-A., Gousenbourger, P.-Y., Striewski, P., and Wirth, B. (2016). Differentiable piecewise-bézier surfaces on riemannian manifolds. *SIAM Journal on Imaging Sciences*, 9(4):1788–1828.
- Benamou, J.-D. and Brenier, Y. (2000). A computational fluid mechanics solution to the monge-kantorovich mass transfer problem. *Numerische Mathematik*, 84(3):375–393.
- Benamou, J.-D., Gallouët, T. O., and Vialard, F.-X. (2019). Second-order models for optimal transport and cubic splines on the wasserstein space. *Foundations of Computational Mathematics*, 19(5):1113–1143.
- Chen, Y., Conforti, G., and Georgiou, T. T. (2018). Measure-valued spline curves: An optimal transport viewpoint. *SIAM Journal on Mathematical Analysis*, 50(6):5947–5968.

- Chewi, S., Clancy, J., Gouic, T. L., Rigollet, P., Stepaniants, G., and Stromme, A. J. (2020a). Fast and smooth interpolation on wasserstein space. *arXiv preprint arXiv:2010.12101*.
- Chewi, S., Maunu, T., Rigollet, P., and Stromme, A. J. (2020b). Gradient descent algorithms for bures-wasserstein barycenters. In *Conference on Learning Theory*, pages 1276–1304. PMLR.
- Chizat, L. (2017). *Unbalanced optimal transport: Models, numerical methods, applications*. PhD thesis, PSL Research University.
- Chizat, L., Peyré, G., Schmitzer, B., and Vialard, F.-X. (2018). Scaling algorithms for unbalanced optimal transport problems. *Mathematics of Computation*, 87(314):2563–2609.
- Gigli, N. (2012). *Second Order Analysis on $(\mathcal{P}_2(M), W_2)$* . American Mathematical Soc.
- Gousenbourger, P.-Y., Massart, E., and Absil, P.-A. (2019). Data fitting on manifolds with composite bézier-like curves and blended cubic splines. *Journal of Mathematical Imaging and Vision*, 61(5):645–671.
- Kondratyev, S., Monsaingeon, L., Vorotnikov, D., et al. (2016). A new optimal transport distance on the space of finite radon measures. *Advances in Differential Equations*, 21(11/12):1117–1164.
- Lavenant, H., Zhang, S., Kim, Y.-H., and Schiebinger, G. (2021). Towards a mathematical theory of trajectory inference. *arXiv preprint arXiv:2102.09204*.
- Liero, M., Mielke, A., and Savaré, G. (2016). Optimal transport in competition with reaction: The hellinger–kantorovich distance and geodesic curves. *SIAM Journal on Mathematical Analysis*, 48(4):2869–2911.
- Liero, M., Mielke, A., and Savaré, G. (2018). Optimal entropy-transport problems and a new hellinger–kantorovich distance between positive measures. *Inventiones mathematicae*, 211(3):969–1117.
- Lisini, S. (2007). Characterization of absolutely continuous curves in wasserstein spaces. *Calculus of variations and partial differential equations*, 28(1):85–120.
- Maniglia, S. (2007). Probabilistic representation and uniqueness results for measure-valued solutions of transport equations. *Journal de mathématiques pures et appliquées*, 87(6):601–626.
- Otto, F. (2001). The geometry of dissipative evolution equations: the porous medium equation.
- Peyré, G., Cuturi, M., et al. (2019). Computational optimal transport: With applications to data science. *Foundations and Trends[®] in Machine Learning*, 11(5-6):355–607.
- Pooladian, A.-A. and Niles-Weed, J. (2021). Entropic estimation of optimal transport maps. *arXiv preprint arXiv:2109.12004*.

Schiebinger, G., Shu, J., Tabaka, M., Cleary, B., Subramanian, V., Solomon, A., Gould, J., Liu, S., Lin, S., Berube, P., et al. (2019). Optimal-transport analysis of single-cell gene expression identifies developmental trajectories in reprogramming. *Cell*, 176(4):928–943.